AIAA-2018-2048

Conditional Studies of the Wake Dynamics of Hemispherical Turret Using PSP

Stanislav Gordeyev[1], Nicholas De Lucca[2], Jacob Morrida[3], Eric J. Jumper[4]
University of Notre Dame, Notre Dame, IN, 46556

and

Donald J. Wittich[5]
Air Force Research Laboratory, Directed Energy Directorate, Kirtland AFB, NM 87117

Fast-response Pressure-Sensitive Paint (PSP) was used to study the wake response of the hemispherical turret at different subsonic and transonic Mach numbers to different pressure patterns on the hemisphere itself. POD technique was used to extract dominant spatial modes and the corresponding temporal coefficients of the unsteady pressure field on the hemisphere. The unsteady pressure distributions in the wake for different conditional events, such as large positive or negative temporal coefficients for different hemisphere-only POD modes, were computed and analyzed. It was found that the wake has the two main dynamic modes, the "switching" and "breathing" ones. The wake dynamics was found to be coupled with the instantaneous location of the separation line on the hemisphere. In the range of tested Mach numbers, the presence of the unsteady shock on the hemisphere did not have any significant effect of the wake dynamics.

I. Introduction

THERE are many directed energy and free-space communications applications requiring to have airborne systems. As a system of choice for these applications, hemispherical turrets with a large field-of-regard are often used. In recent years, there has been extensive experimental work to characterize both the aerodynamic [1-3] and aero-optic [4-6] performance of these turrets. Also, there have been several CFD studies of the flow around hemispherical turrets [7-11].

Al low subsonic speeds, the flow around the hemisphere is fully subsonic. At Mach numbers above 0.55, the flow over a hemisphere becomes locally supersonic, with a terminating unsteady shock forming near the apex of the hemisphere [6]; the shock oscillates within a few degrees of the apex [12-14]. Due to high density gradients associated with the shock it results in an increased amount of aero-optical distortions at side-looking angles. One way to mitigate this problem is to use adaptive optics approach [15]; however, the instantaneous wavefronts, which depend on the shock location and strength, must be known. To predict these shock properties, the flow dynamics

[1] Associate Professor, Department of Aerospace and Mech. Eng., AIAA Associate Fellow
[2] Post-Doctoral Researcher, Department of Aerospace and Mech. Eng., Student AIAA Member
[3] Graduate Research Assistant, Department of Aerospace and Mech. Eng., Student AIAA Member
[4] Professor, Department of Aerospace and Mech. Eng., AIAA Fellow
[5]Aerospace Engineer, Laser Division, 3550 Aberdeen Ave SE, AIAA Senior Member

around the hemisphere at transonic speeds must be better understood to provide means of passive/active optical mitigation strategies.

Optical and pressure measurements in both flight and tunnel tests indicate that at transonic speeds there is a coupling between the shock and the wake motion [16-20]. Recent advances in fast-response Pressure Sensitive Paint (PSP) allows studying a full spatio-temporal pressure field on and around the turret. PSP measurements are based on oxygen-sensing molecules known as luminophore, which fluoresce when exposed to ultraviolet light [21,22]. Oxygen quenches the luminescence of the paint, so as the air pressure increases, the oxygen concentration increases, which reduces the light emission. Therefore, the paint fluorescence intensity gets brighter as pressure decreases.

The pressure field around turrets has been studied in the past using PSP [3,23-25]. The surface pressure field on the turret carries both the signature of the turbulent structures in the turret's vicinity and any global pressure motion (modes) over the turret. Both the global pressure modes and the turbulent structures have been shown to affect the optical performance of the turret [4-6]. Also, the unsteady pressure-induced loading introduces aero-mechanical effects, which leads to additional unwanted beam jitter [26]. Thus, by studying the pressure environment over the turret, a better understanding of the flow features affecting optical performance can be gained and the design of optical turrets can potentially be improved.

In previous aforementioned PSP studies, the pressure field only on the turret itself was measured and studied. Based on these and complimentary optical studies, different dynamical responses of the wake downstream of the turret were proposed [26]. These wake motions were speculated to be responsible for most of aero-optical effects at downstream-looking angles.

In this paper, the unsteady pressure field on and around the hemispherical turret was studied using fast-response PSP. Using measured global pressure fields, different dominant pressure modes on the hemisphere only were extracted using Proper Orthogonal Decomposition (POD) [27-29]. Using a conditional analysis, wake responses to these dominant hemisphere-only modes were extracted and discussed. It was demonstrated that the extracted wake responses are consistent with the ones, previously proposed in [26]. This analysis provides a better understanding the wake dynamics at high subsonic and transonic speeds.

A companion paper [30] uses the same experimental data to alternatively study the dominant flow features using POD and Dynamic Mode Decomposition (DMD) techniques.

II. Experimental Setup

This experiment was performed in the Whitefield wind tunnel facility at the University of Notre Dame. This is a 3'x3'wind tunnel facility that is capable of up to M = 0.6 flow. A contraction was placed in the facility to increase a maximum freestream Mach number up to M = 0.7. Two different models were studied in this experiment, shown in Figure 1, radius R = 5" hemisphere and R = 4" hemisphere; results for R = 4" hemisphere only will be presented in this paper. A schematic and picture of the setup are shown in Figure 2. Polymer-ceramic/PtTFPPF PSP formulation, manufactured by ISSI Inc. and demonstrated to provide high, faster than 10 kHz, response [31], was applied on and around the turret; the paint has a pinkish color and can be seen in Figure 1, right. To illuminate PSP, eight UV light sources, emitting in a narrow band about 400 nm, were placed on both sides of the test section. The UV lights were aligned with quartz inserts in the tunnel, as seen in Figure 2, to minimize UV light losses through optical windows. The PSP images were taken using three Phantom high speed cameras. The three cameras, Figure 2, used were a v1611 (Camera 1), a v1610 (Camera 2) and a v711 (Camera 3). Additionally, a set of 10 PSI

differential Kulite sensors were placed both on the turret and in the wake to verify the PSP and perform an in-situ calibration.

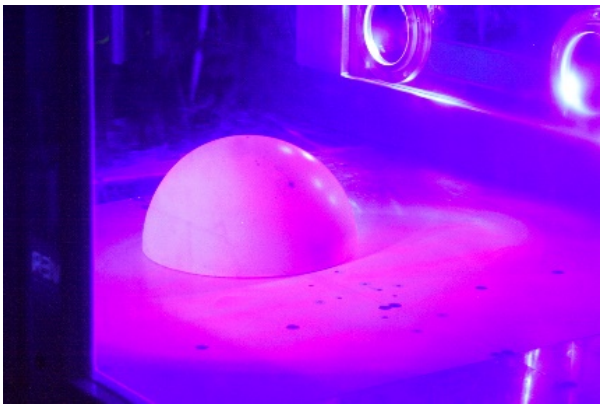
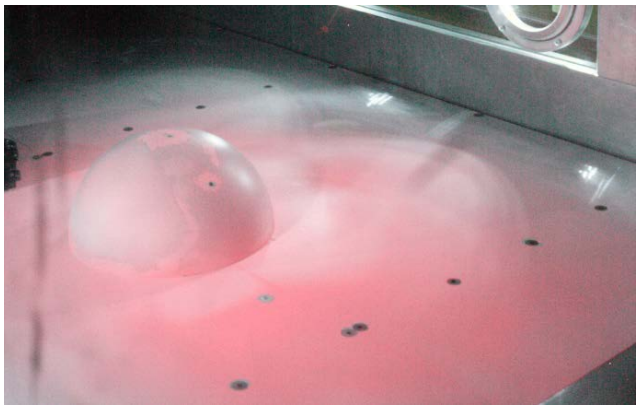

Figure 1: The tested turret geometries. Left is the 10” hemisphere. Right is the 8” hemisphere.

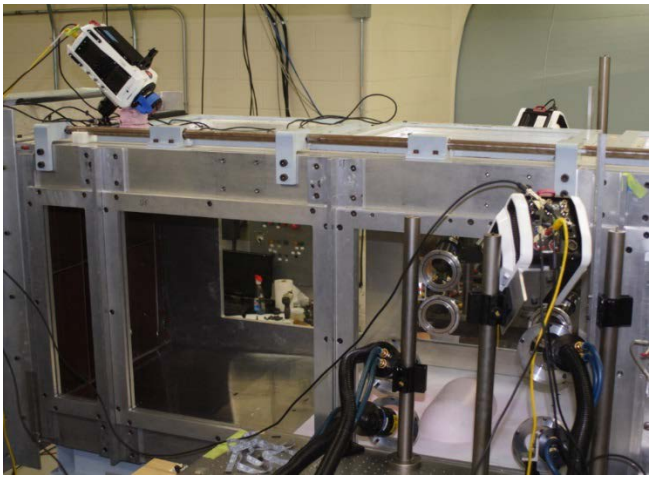
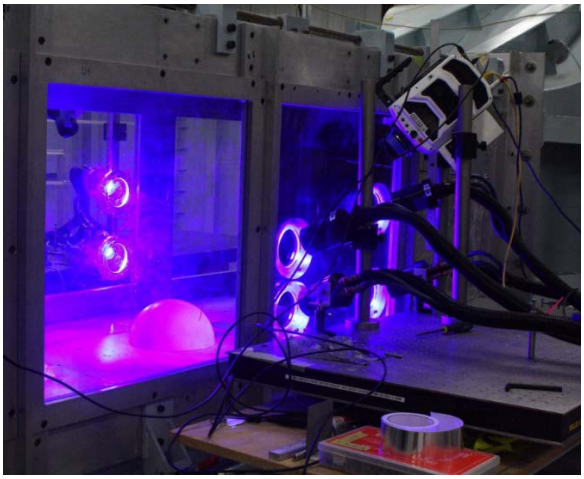

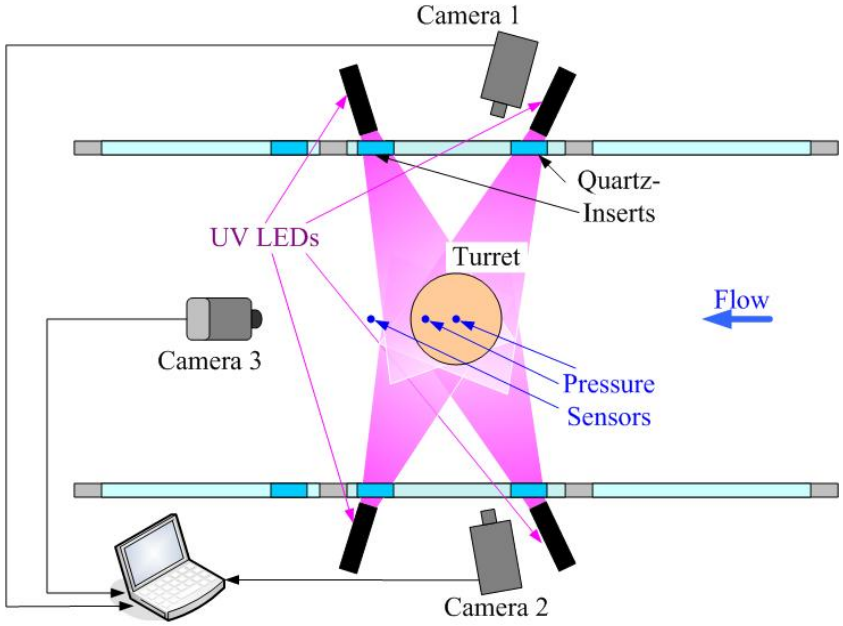

Figure 2: Pictures (top) and a schematic (bottom) of the experimental setup.

The tunnel was run at various Mach numbers between M = 0.4 and M = 0.66. Data were acquired at two different sample rates. The first sampling rate was 3 kHz for total of 32000 frames for all three cameras. The second one was 10 kHz for total of 30000 frames for cameras 1 and 2. Because it was an older model, for the second sampling rate camera 3 was set to a lower sample rate of 2.5 kHz. The Kulite data were acquired at 30 kHz. The three cameras were triggered simultaneously and the internal clocks were also synchronized. The Kulites were also triggered simultaneously with the cameras.

III. Data Analysis

Before analysis was done with the PSP images, the Kulite pressure sensors were used to calibrate the paint response in-situ. This was done by first extracting a small patch, 10 pixel x 10 pixel, of intensity data near a pressure port and spatially averaging to reduce noise, then comparing it to the pressure output from the Kulite. The known linear relationship between the intensity, $I(t)$, and pressure, $P(t)$, is given by

$$\frac{\overline{I(t)}}{I(t)} = 1 + A \cdot P(t) \tag{1}$$

where the overbar indicates a time averaged quantity, and P is the *mean-removed* unsteady pressure. The variable A is a constant which was found by applying a linear fit to the normalized intensity ratio vs mean removed pressure. The paint was found to correctly resolve the unsteady pressure spectrum up to a frequency around 500 Hz, see Figure 3. The paint response is expected to be faster than 10 kHz, but above 500 Hz pressure fluctuations were smaller than PSP sensitivity, resulting in a flat noise-dominated part of the spectrum.

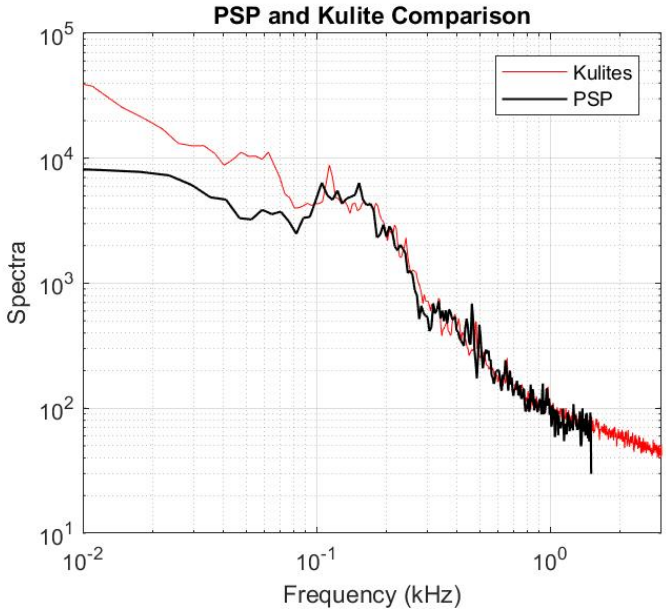

Figure 3: Power Spectra of the Pressure based on the Kulite (blue) and PSP (red) on top of the turret.

After converting the images into respective pressure fields, the data from all three cameras were used to reconstruct the full unsteady pressure field on the surface of the hemisphere and around it on the tunnel wall, using Perspective Transformation Matrix (PTM) approach [3].

Proper Orthogonal Decomposition (POD) was used to both reduce the experimental noise and to analyze the data at different Mach numbers. To compute POD modes and corresponding temporal coefficients, a widely-accepted algorithm using a Singular Value Decomposition (SVD) was used [32].

Pressure field on the hemisphere only, $P_H(\vec{x},t)$, was decomposed onto a set of orthogonal spatial POD modes, $\{\varphi_n(\vec{x})\}$, and the corresponding temporal coefficients, $\{a_n(t)\}$, as $P_H(\vec{x},t) = \sum_n a_n(t)\varphi_n(\vec{x})$. For the first several dominant modes, conditional events were considered, when the corresponding temporal coefficients were either largely positive, $a_n(t) > C_n$, or negative, $a_n(t) < -C_n$. The threshold value, C_n, was chosen to be a standard deviation of the corresponding temporal coefficient, $C_n = a_{rms}$. For both Mach numbers, the conditionally-averaged spatial variations of the pressure fields on the hemisphere and in the separated wake were computed during these conditional events,

$$\text{Conditional } P_{rms}(\vec{x}) = \left\langle P(\vec{x},t)^2 \mid a_n(t) > C_n \text{ or } a_n(t) < -C_n \right\rangle^{1/2}.$$

The system of coordinates originates at the center of the hemisphere, with x-, y- and z-coordinates being the streamwise, the cross-stream and the wall-normal directions, respectively. X-values increase downstream and z-values increase away from the wall.

IV. Results

Figure 4 shows normalized temporal standard variations of the unsteady pressure field on and around the hemisphere for subsonic, M = 0.55 case, Figure, 4, left, and transonic, M = 0.66 case, Figure 4, right. As the images from Camera 3 were found to have insufficient intensity variations to correctly reconstruct pressure fields, data only from Cameras 1 and 2 were used to reconstruct the pressure field. As a consequence, it resulted in "no-data" region on the downstream portion of the hemisphere, shown as a dark blue wedge region in Figure 4.

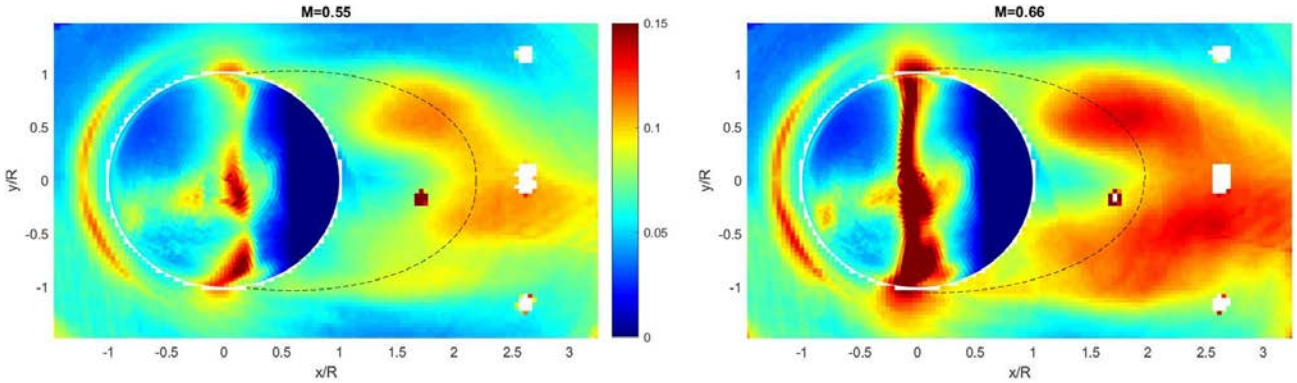

Figure 4. Temporal standard variation of the pressure field around the hemisphere for incoming M = 0.55 (left) and M = 0.66 (right). Flow goes from left to right. Pressure variations are normalized by the incoming dynamic pressure, spatial coordinates are normalized by the hemisphere radius, R. The boundary of the recirculation region downstream of the hemisphere, measured in [18], is outlined by a dashed line.

The unsteady pressure field on the hemisphere is dominated by the separation-related phenomenon, seen as regions of increased pressure fluctuations on both sides of the hemisphere near x = 0. The necklace vortex is present as a thin line in front of the hemisphere and the "footprint" of the turbulent wake is seen downstream of the hemisphere, between x/R = 1 - 3. In [18] the topology of the wake was studied using oil-flow visualization technique and the approximate extent of the recirculation region downstream of the hemisphere is also plotted in Figure 4 as a dotted line. The region of the increased pressure fluctuations approximately coincides with the boundary of the recirculation region. Thus, later in this paper the location of this region of the increased pressure variations will be used to estimate the position and the size of the recirculation region.

At the transonic speed of M = 0.66 the unsteady shock forms near the apex of the hemisphere and the increased pressure fluctuations due to the unsteady shock at x = 0 are clearly seen in Figure 4, right. Also, the wake-related pressure intensity is slightly larger for M = 0.6 than for M = 0.55.

For both Mach numbers, the wake is not totally symmetric in the spanwise direction, as the part of the wake for the positive y-locations is stronger than for the negative y-locations. As the pressure field at the positive and the negative y-locations were reconstructed using images from two different cameras, this asymmetry might be related to the different values of the calibration A-constants in Eq. (1); also, it might be related to a possible small asymmetry in the hemisphere location in the spanwise direction, relative to the tunnel walls.

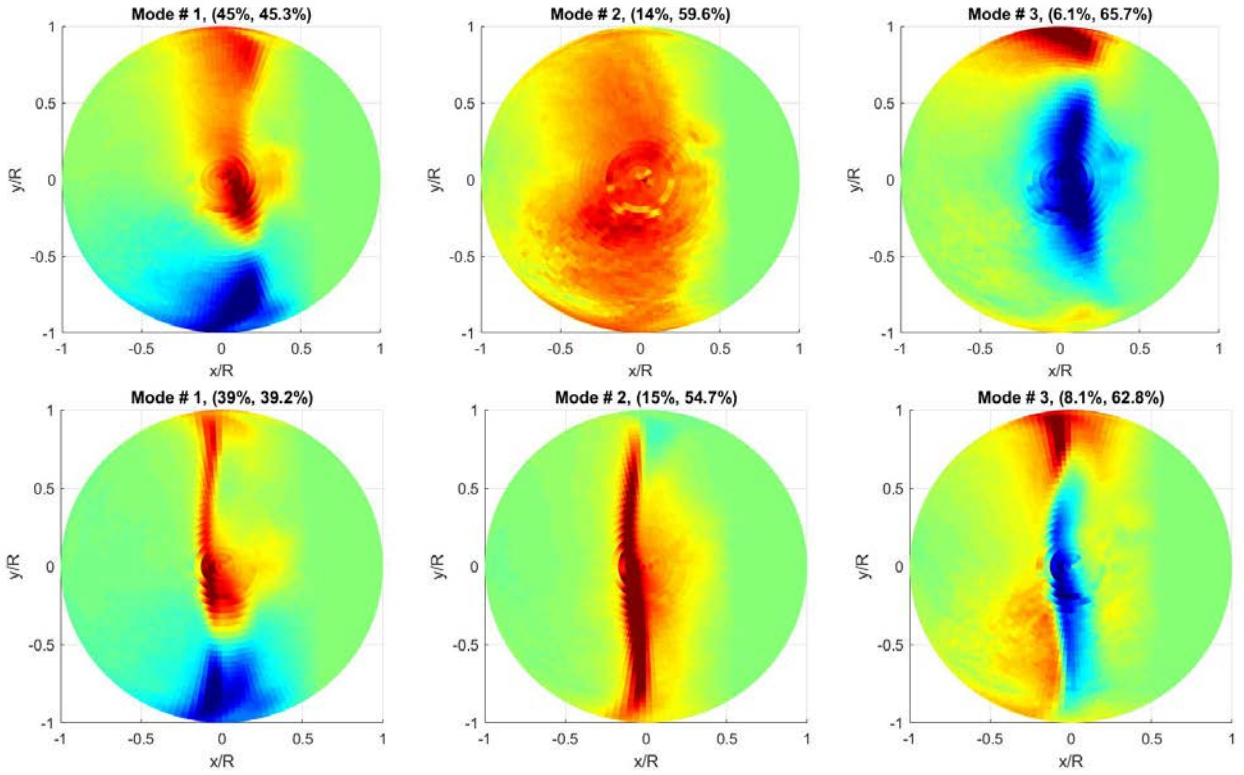

Figure 5. First three dominant hemisphere-only POD modes for M = 0.55 (top row) and for M = 0.66 (bottom row). The first number in parentheses indicates a relative mode energy, the second number indicates the total amount of energy up to and including the mode). Flow goes from left to right.

The first three dominant spatial hemisphere-only POD modes for M = 0.55 are shown in Figure 5, top row. These modes collectively are responsible for 64% of the total fluctuation pressure "energy". The first mode holds 45% of the pressure "energy" and is predominantly anti-symmetric in the spanwise direction. The second and the third modes are symmetric in the spanwise direction. Most of the pressure variations in these first modes are near or upstream of the separation line, which is approximately located at x/R = 0.2 [18]. Overall, these POD modes are very similar to the POD modes, observed on a hemisphere-on-cylinder turret for M = 0.4 [3].

The first three hemisphere-only POD modes for transonic incoming Mach number of 0.66 are shown in Figure 5, bottom row. As the separation line is significantly affected by the presence of the unsteady shock, most of the spatial variations of the POD modes are concentrated along the line about x = 0. The first mode is also mostly axisymmetric in the spanwise direction and holds approximately 38% of the "energy", while both the second and third modes are symmetric in the spanwise direction. The first three POD modes capture 62% of the pressure "energy". Thus, the main difference between the subsonic and transonic POD modes is the more spatially-localized pressure variations due to the shock presence at higher transonic Mach number.

Power spectra of the corresponding temporal coefficients for the first three POD modes are shown in Figure 6. At the lower Mach number of 0.55, Figure 6, left, the spectra are exhibit significant low-frequency content, $St_D < 0.3$; the spectra were found to be similar to the spectra of the first POD modes around the hemisphere-on-cylinder turret [3].

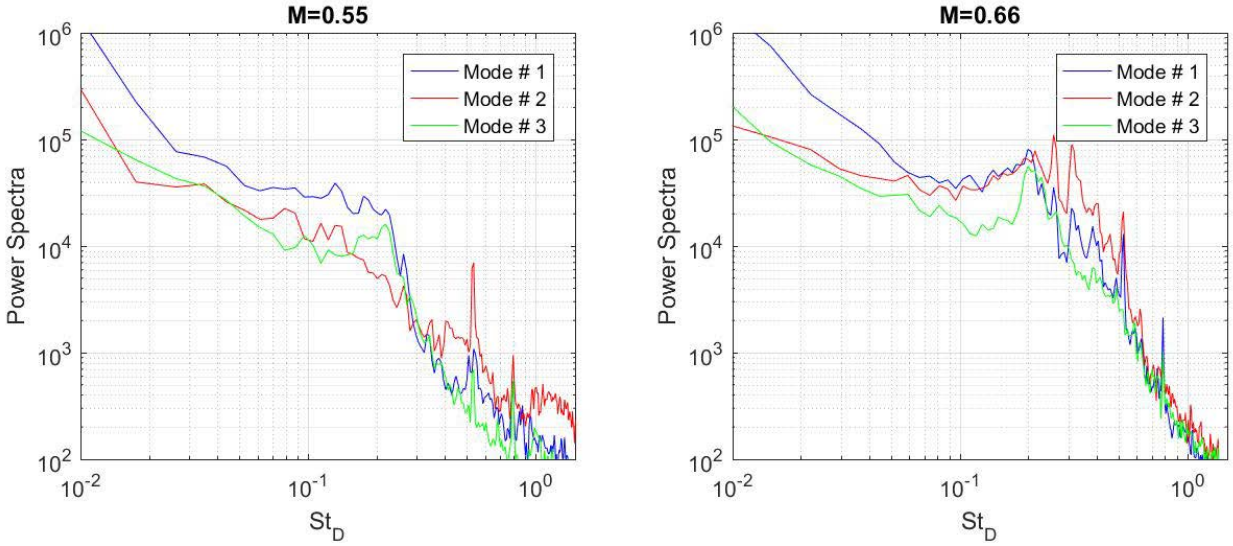

Figure 6. Power spectra for the temporal coefficients of first 3 hemisphere-only POD modes for M = 0.55 (left) and for M = 0.66 (right).

The spectra for the higher Mach number of 0.66 are shown in Figure 6, right. Spectra for Modes # 1 and # 3 have a distinct peak near $St_D = 0.2$. This peak is related to the unsteadiness of the separation line over a hemisphere, observed in both aero-optical and local pressure data at similar transonic Mach numbers [6]; the similar peak was observed in unsteady pressure spectra for hemisphere-on-cylinder turrets [3]. Mode # 2, in addition to having the main peak at $St_D = 0.2$, also has additional peaks near $St_D = 0.3$. Similar distinct peaks at the same range of the normalized frequencies were observed in wavefront spectra in-flight for side-viewing angles for M = 0.7 for both the hemisphere-on-cylinder [13] and hemisphere-only turrets [6] and were contributed to the

unsteadiness of the shock near the apex of the hemisphere. Mode # 2 at this Mach number is essentially non-zero only in the narrow region near apex of the hemisphere, see Figure 5, middle bottom plot, confirming that it is mostly related to the unsteady shock.

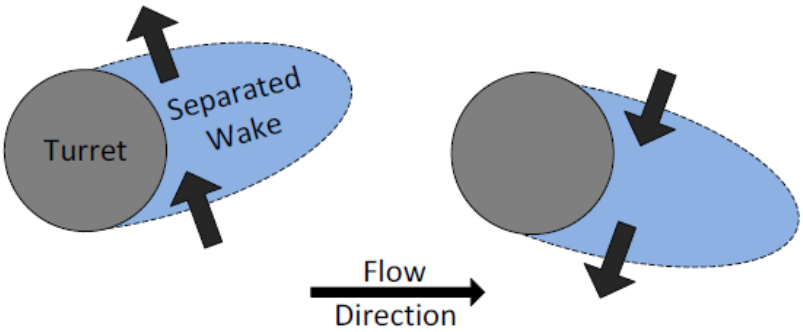

Figure 7. Wake "shifting" mode. From [26].

In [26] it was speculated, based on the analysis of simultaneous pressure and aero-optical measurements, that the dynamics of the separation region downstream of the turret is coupled with the pressure variations on the turret. Two main wake dynamic types of motion were proposed, the wake "shifting" mode, schematically depicted in Figure 7 and the wake "breathing" mode, shown in Figure 8.

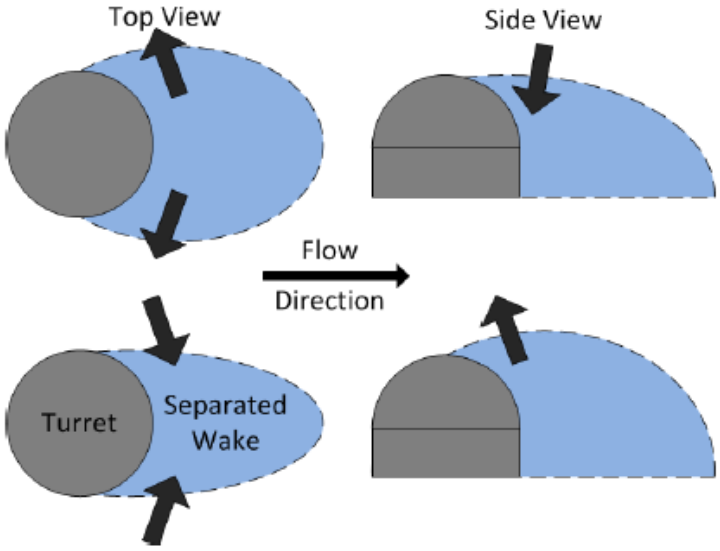

Figure 8. Wake horizontal (left column) and vertical (right column) "breathing" modes. From [26].

Figure 9 illustrates the relationship between the temporally-evolving mean-removed pressure field and the unsteady separation location. The time-averaged pressure distribution over a curved surface, such as a hemisphere, is shown as a dashed line. The flow accelerates at the front portion of the hemisphere, so the pressure decreases. After passing the apex, the flow starts slowing down and the pressure begins to raise, resulted in the adverse pressure gradient environment. At some point, the flow separates and the pressure becomes approximately constant inside the separation region. Let's say at some moment the separation point moves upstream of the time-averaged separation location. As a consequence, the pressure distribution upstream of the separation line

will adjust itself to reach the constant pressure value further upstream. As shown in Figure 9, it will result in a positive pressure deviation near the instantaneous separation line from the time-averaged pressure distribution, which is by definition a mean-removed pressure fluctuation. So, a positive pressure fluctuations near the separation line should correspond to upstream shift of the separation line. This shift would result in a larger separation bubble, as schematically shown in the insert in Figure 9. For the same reasoning, the negative pressure fluctuations would correspond to the downstream motion of the separation line and a smaller separation bubble.

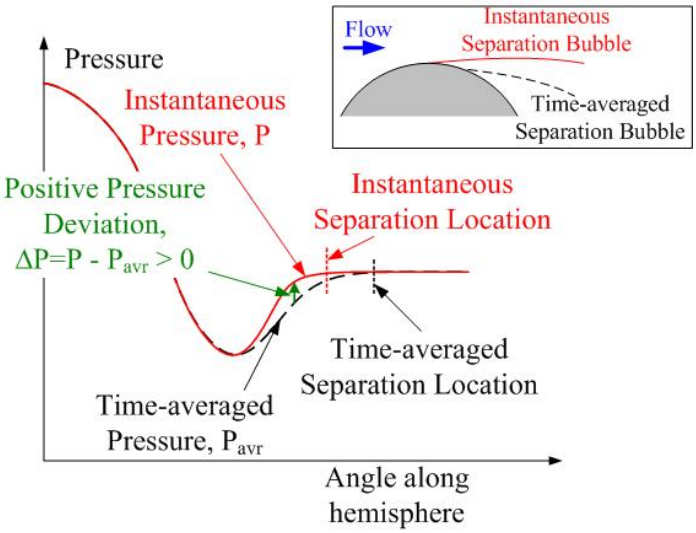

Figure 9. Relationship between the time-varying pressure distribution and the location of the unsteady separation point.

From this prospective, the first hemisphere-only POD mode in Figure 5 can be interpreted as simultaneous shifts in the separation line in opposite directions: when the separation line on the top portion (positive y-location) of the turret advances upstream, the separation line on the bottom portion (negative y-location) retreats downstream. The magnitude of the temporal coefficient describes the amount of this shift. Negative values of the temporal coefficient would result in a sign change of the POD mode, indicating that the separation lines would move in the opposite directions, compared to the case with the positive temporal coefficient. The described motion of the separation line corresponds to the proposed wake "shifting" motion, shown in Figure 7. Thus, the first hemisphere-only POD mode is related to the wake "shifting" mode.

Consequently, the second hemisphere-only POD mode is symmetrical in the spanwise direction, with the positive values close the hemisphere apex. It should correspond to a simultaneous advance or a retreat of the separation line, which is a vertical "breathing" wake motion, shown in Figure 8, and this separation line motion should affect the size of separation region. Finally, the third hemisphere-only POD mode is symmetrical, with large positive regions on both sizes of the hemisphere near the wall and a negative region near the top of the hemisphere. It would correspond to a situation, when on both sides of the hemisphere the separation line advances upstream and forcing the wake to become wider near the surface, while the portion of the separation line near the top retreats downstream, making the separation region "flatter". From Figure 8, it can be interpreted as simultaneous horizontal and vertical wake "breathing" motion.

To study the actual wake response to various modal pressure distributions on the hemisphere, a conditional analysis was performed, as outlined previously. Conditionally-averaged spatial variations of pressure for large positive and for large negative temporal coefficients for the first hemisphere-only POD mode are shown in Figure 10, top and middle rows, correspondingly. The conditional spatial pressure variations along a line x/R = 2 are plotted in Figure 10, bottom row, along with the unconditional spatial pressure variations. The left column corresponds to M = 0.55 and the right column corresponds to M = 0.66. Indeed, the wake was found to be shifting in the spanwise direction for both the large positive and the large negative values of the a_1-coefficient. When the separation line advances on the positive y-side of the hemisphere (which corresponds to a positive temporal coefficient), the wake shifts in the positive y-direction and when the separation line retreats on the positive-y side of the hemisphere, the wake shifts in the negative y-direction. Despite the presence of the unsteady shock at M = 0.66, the wake topology seems to be largely unchanged, compare the left and right columns in Figure 10. Thus, the presence of the "shifting" wake mode, proposed in [26] and depicted in Figure 7, is confirmed and this mode is correlated to the first hemispherical POD mode. At x/R = 2, the wake shifts by as much as $\Delta y/R = \pm 0.2$ in the spanwise direction from its unconditionally-averaged location.

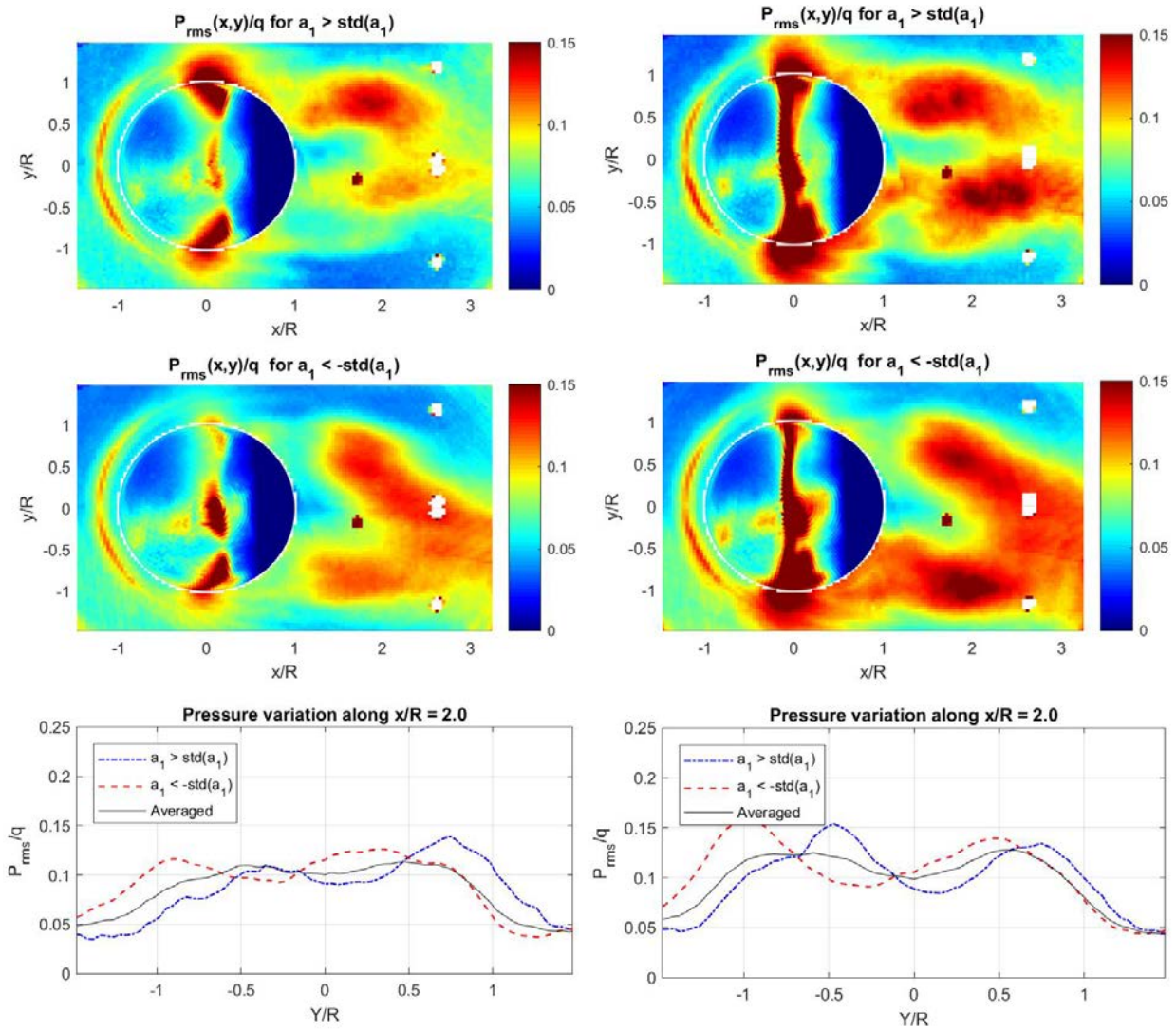

Figure 10. Conditionally averaged pressure variations for large positive (top) and negative (middle) coefficients for the first POD mode for M = 0.55 (left column) and for M = 0.66 (right column). Bottom plots shows the conditionally-averaged spatial pressure variation along X/R = 2 line.

Temporal evolutions of the temporal coefficients of the first hemisphere-only POD mode for both Mach numbers are presented in Figure 11. For both Mach numbers, the coefficients exhibit a bi-modal distribution, when they are either largely positive or largely negative, with random switching between. Analysis of the pressure fields collected in flight [33] did not reveal any switching in the first POD mode, and neither was it observed in LES-based numerical simulations of the flow around turrets at subsonic speeds [34,35]. One possible reason for this switching behavior is the presence of the tunnel walls, which might make the symmetric wake topology unstable in favor of the becoming-stable shifted wake topologies. This potential tunnel-related enhancement of the wake motion should be considered when the tunnel-based experiments are compared with flight tests or numerical simulations.

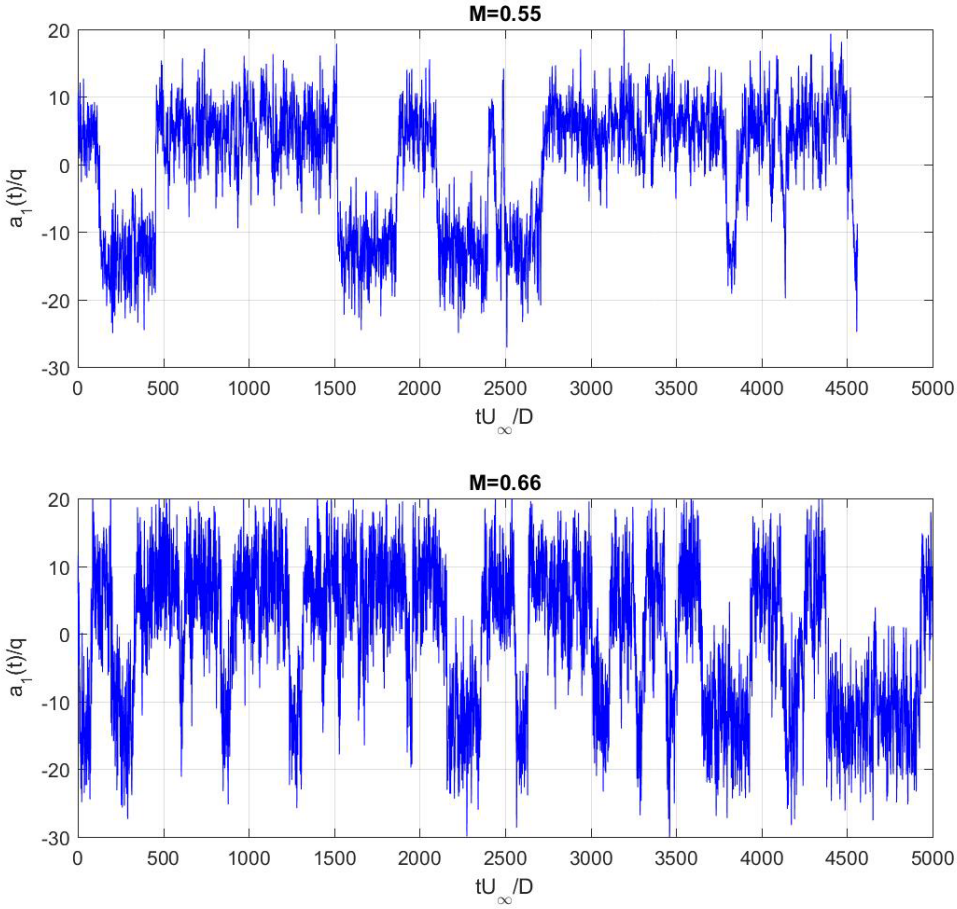

Figure 11. Time series of the temporal coefficients for the first hemisphere-only POD mode for M = 0.55 and 0.66.

As discussed before, the second hemispherical POD mode corresponds to the case, when the separation line moves symmetrically either forward or backward on the turret. It should corresponds to the vertically "breathing" mode, shown in Figure 8, right column, it should result the streamwise extent of the separation region. However, the conditional analysis of the wake response, shown in Figure 12, does not reveal any significant changes in the wake extent in the streamwise direction. Rather, this mode is related to different levels of the pressure variations near the re-attachment region. When the separation line moves forward, corresponding to the positive a_2-values, the pressure fluctuations are decreased in the wake and vice versa. Again, the presence of the unsteady shock does not affect the topology of the separated region.

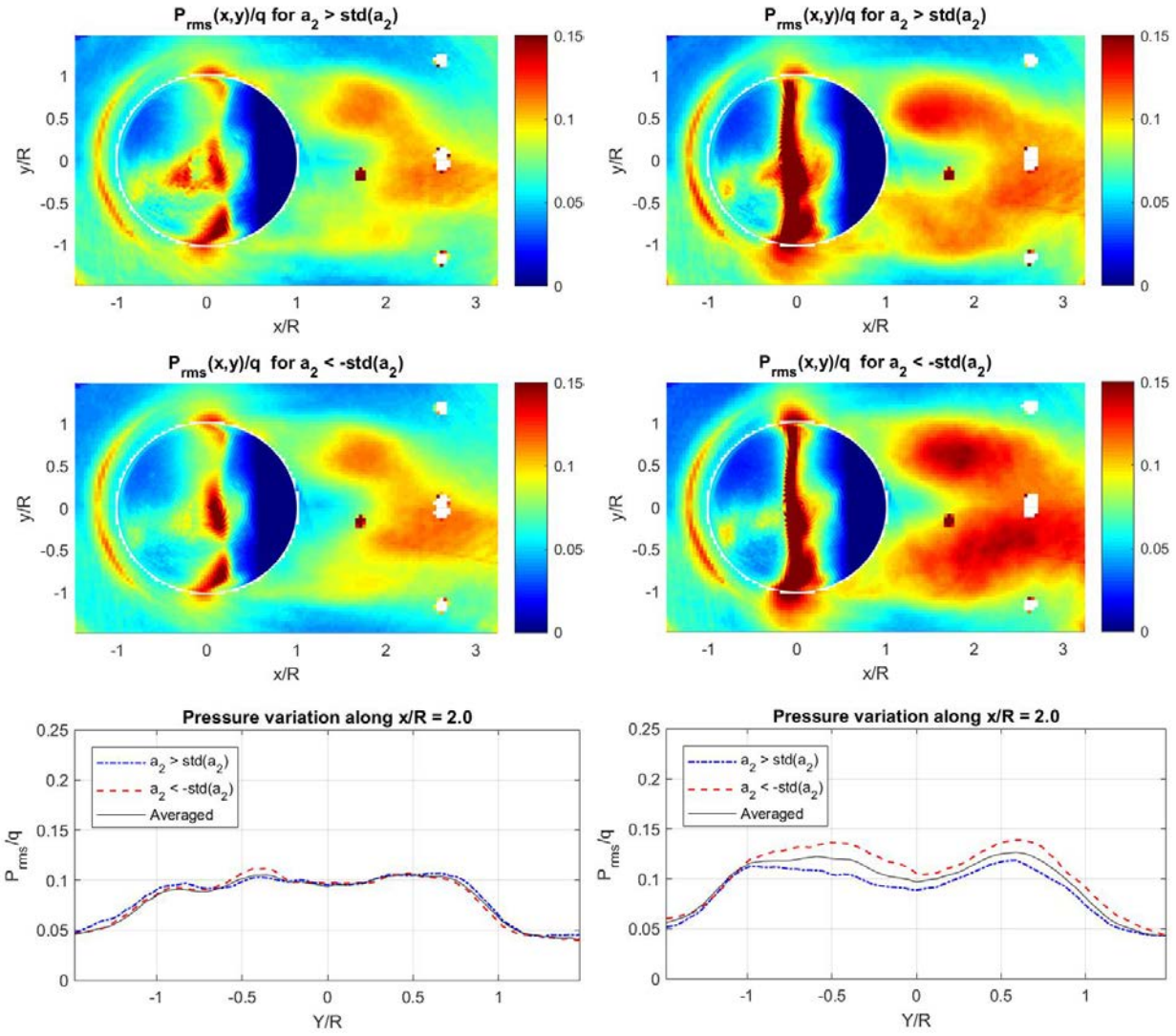

Figure 12. Conditionally averaged pressure variations for large positive (top) and negative (middle) coefficients for the second POD mode for M = 0.55 (left column) and for M = 0.66 (right column). Bottom plots shows the conditionally-averaged spatial pressure variation along X/R = 2 line.

The third POD corresponds to the case, when the separation line near the hemisphere base moves in one streamwise direction, while near the top of the hemisphere it moves in the opposite direction. Conditionally-averaged pressure variations, related to the third POD mode, indicate that the wake response resembles the horizontally "breathing" mode, as schematically shown in Figure 8, left column. When the separation line moves upstream near the bottom of the turret and retreats near the top (corresponding to a positive temporal coefficient), it results in the wake widening in the spanwise direction, see Figure 13, left column. Conversely, then the separation moves downstream near the bottom of the hemisphere, the wake shrinks in the spanwise direction. The shock presence intensifies the pressure fluctuations in the wake, compare top and bottom rows in Figure 13.

Thus, these conditional studies do indicate that the wake dynamics is correlated with the dominant pressure modes on the hemisphere. It confirms that both the "shifting" and horizontal "breathing" modes are present in the wake dynamics. The presence of the unsteady shock at transonic speeds does not significantly affect the wake dynamics, at least in the range of Mach number tested. It agrees with similar findings based on the analysis of the aero-optical performance of the wake at subsonic and transonic speeds [6,13].

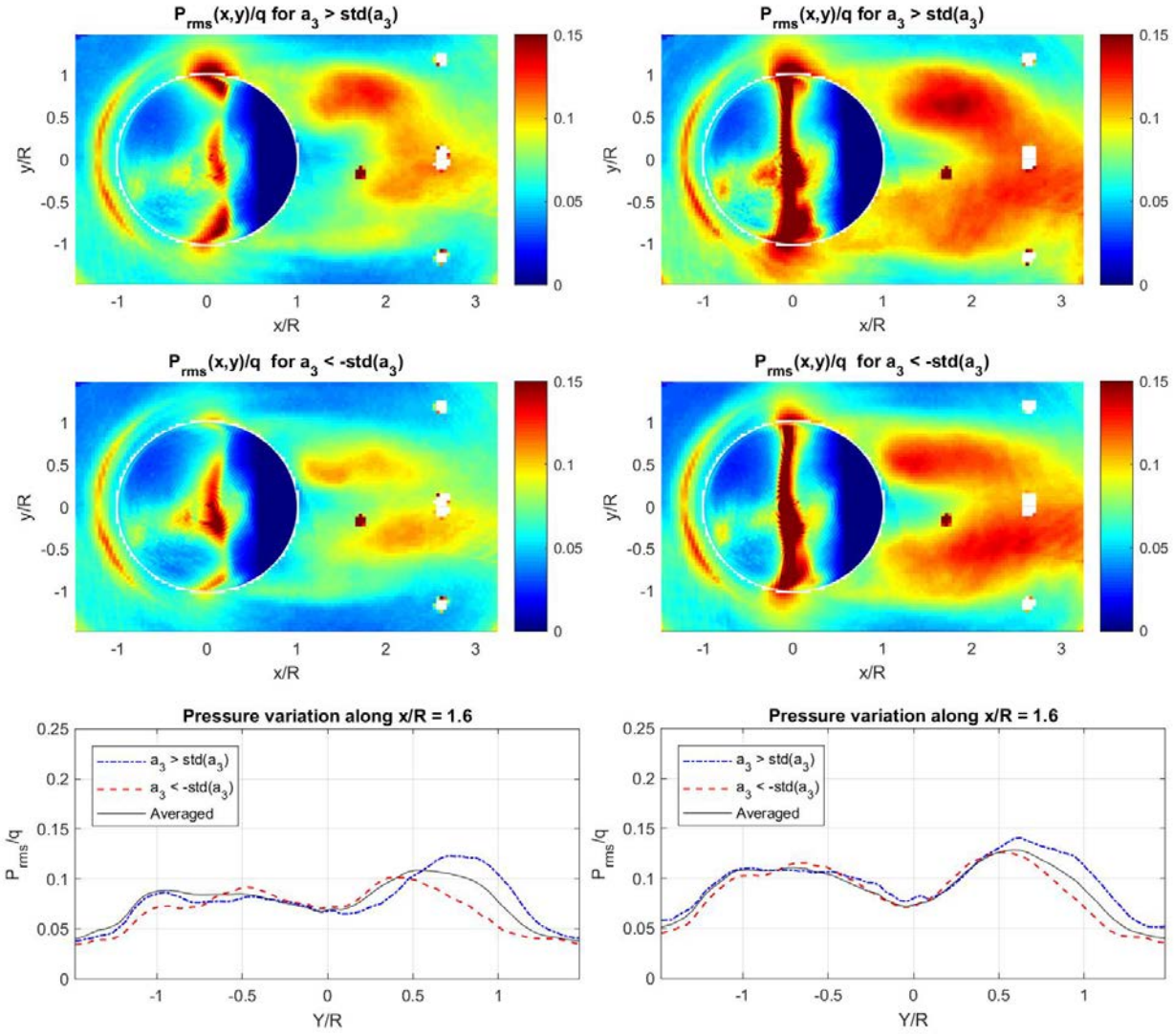

Figure 13. Conditionally averaged pressure variations for large positive (top) and negative (middle) coefficients for the third POD mode for M = 0.55 (left column) and for M = 0.66 (right column). Bottom plots shows the conditionally-averaged spatial pressure variation along X/R = 1.6 line.

V. Conclusions

Spatio-temporal unsteady pressure fields on the surface of and around a hemispherical turret for incoming Mach numbers of 0.55 and 0.66 were experimentally studied using a fast-response

pressure-sensitive paint. Previous experiments focused on the unsteady pressure distributions only on the turret surface. The region of the increased pressure fluctuations downstream of the turret was found to coincide with the boundary of the separation region. The increase of the pressure fluctuations on the turret was also associated with the instantaneous location of the separation line. Assuming that the separation and the re-attachment lines are always characterized by the local increase in the surface pressure fluctuations, obtaining global time-resolved pressure fields on and around the turret allowed studying the global dynamics and instantaneous extent of the separated region downstream of the turret and its relation to the separation line of the turret. To accomplish this, pressure field on the turret only was decomposed into spatial POD modes and the corresponding temporal coefficients. The first POD mode was found to by anti-symmetric in the spanwise direction. This mode was interpreted as simultaneous 180-degree out-of-phase motion of the separation line on the opposite spanwise sides of the turret; that is when the separation line advances on one side of the turret, the separation line retreats on the other side of the turret, and vice versa. The second POD mode was spanwise symmetric and it was associated with the separation line of the turret simultaneously moving either forward or backward. The third POD mode was also spanwise symmetric and corresponded to the situation, when the separation line on both sides of the turret moves upstream, while the separation line on top of the turret moves downstream and vice versa.

To study whether these local movements of the separation line on the turret are correlated with the global motion of the separation region downstream of the turret, the unsteady pressure field was conditionally averaged for either large positive or large negative temporal coefficients of the corresponding POD mode. The first POD mode was found to be correlated with a spanwise shift of the separated region as a whole, the so-called wake “shifting”. The third POD mode was found to correspond to the separation region been either wider or narrower in the spanwise direction, the so-called wake “breathing”. The second POD mode did not have any significant correlation with the motion of the separation region.

At the incoming M = 0.55, the flow was subsonic everywhere around the turret and at higher M = 0.66 the unsteady shock formed near the turret apex. While the shock presence significantly modified POD modes on the turret itself, the conditional response of the separated region was found to be very similar for both Mach numbers. It agrees with aero-optical studies of the separation region downstream of the turret at different subsonic and transonic, up to M = 0.8, speeds, where it also found that the wake dynamics is independent of the incoming Mach numbers. Additional studies at even higher Mach numbers should be conducted to see at what Mach number the unsteady shock on the turret will be sufficiently strong to affect the dynamics of the separation region.

VI. Acknowledgments

This work is supported by the Joint Technology Office, Grant number FA9550-13-1-0001 and by AFRL, Contract number FA9451-13-C-0001. The U.S. Government is authorized to reproduce and distribute reprints for governmental purposes notwithstanding any copyright notation thereon.

The authors also would like to thank Dr. Thomas Juliano from University of Notre Dame for his help painting the models and Steve Palluconi from ISSI, Inc. for many useful discussions and recommendations about using PSP.

References

[1] C.H. Snyder, M.E. Franke, M.L. Masquelier, “Wind-Tunnel Tests of an Aircraft Turret Model”, Journal of Aircraft, 37(3), pp. 368-376, 2000.

[2] R. Sluder, L. Gris, J. Katz, “Aerodynamics of a Generic Optical Turret”, Journal of Aircraft, 45(5), pp. 1814-1815, 2008.

[3] S. Gordeyev, N. De Lucca, E.J. Jumper, K. Hird, T.J. Juliano, J.W. Gregory, J. Thordahl, and D.J. Wittich, “Comparison of Unsteady Pressure Fields on Turrets with Different Surface Features using Pressure Sensitive Paint”, Experiments in Fluids, 55, p. 1661, 2014.

[4] C. Porter, S. Gordeyev, M. Zenk, and E.J. Jumper, "Flight Measurements of the Aero-Optical Environment around a Flat-Windowed Turret”, AIAA Journal, 51(6), pp. 1394-1403, 2013.

[5] N. De Lucca, S. Gordeyev, and E.J. Jumper, "In-flight aero-optics of turrets”, Journal of Optical Engineering, 52(7), 071405, 2013

[6] J. Morrida, S. Gordeyev and E. Jumper, “Transonic Flow Dynamics Over a Hemisphere in Flight”, AIAA Paper 2016-1349, 2016.

[7] E. Mathews, K. Wang, M. Wang and E. Jumper, “LES of an Aero-Optical Turret Flow at High Reynolds Number”, AIAA 2016-1461, 2016.

[8] R. Jelic, S. Sherer and R. Greendyke, “Simulation of Various Turret Configurations at Subsonic and Transonic Flight Conditions Using OVERFLOW”, Journal of Aircraft, 50, pp. 398-409, 2013.

[9] W.J. Coirier, C. Porter, J. Barber, J. Stutts, M. Whiteley, D. Goorskey, and R. Drye, ”Aero-Optical Evaluation of Notional Turrets in Subsonic, Transonic and Supersonic Regimes,” AIAA Paper 2014-2355, 2014

[10] P.E. Morgan and M.R. Visbal, “Hybrid Reynolds-Averaged Navier–Stokes/Large-Eddy Simulation Investigating Control of Flow over a Turret,” Journal of Aircraft, Vol. 49, No. 6, pp. 1700-1717, 2012.

[11] J. Ladd, A. Mani, and W. Bower, “Validation of Aerodynamic and Optical Computations for the Unsteady Flow Field About a Hemisphere-on-Cylinder Turret,” AIAA Paper 2009-4118, 2009.

[12] S. Gordeyev, and E.J. Jumper, “Fluid Dynamics and Aero-Optics of Turrets", Progress in Aerospace Sciences, 46, pp. 388-400, 2010.

[13] J. Morrida, S. Gordeyev, N. De Lucca, E. Jumper, “ Shock-Related Effects on Aero-Optical Environment for Hemisphere-On-Cylinder Turrets at Transonic Speeds,” Applied Optics, 56(16), pp. 4814-4824, 2017.

[14] J. Morrida, S. Gordeyev, E. Jumper, S. Gogineni and D.J. Wittich, “Investigation of Shock Dynamics on a Hemisphere Using Pressure and Optical Measurements,” AIAA Paper 2016-1348, 2016.

[15] Tyson, R. K., Principles of Adaptive Optics, 2nd ed., Academic Press, Chestnut Hill, MA, 1991.

[16] J. Morrida, N. De Lucca, S. Gordeyev, and E.J. Jumper, “Simultaneous Pressure and Optical Measurements Around Hemispherical Turret in Subsonic and Transonic Flight,” AIAA Paper 2017-3654, 2017.

[17] D. J. Goorskey, R. Drye and M. R. Whiteley, “Dynamic modal analysis of transonic Airborne Aero-Optics Laboratory conformal window flight-test aero-optics”, Opt. Eng. 52 (7), 071414, 2013.

[18] S. Gordeyev, A. Vorobiev, E. Jumper, S. Gogineni and D.J. Wittich, "Studies of Flow Topology around Hemisphere at Transonic Speeds Using Time-Resolved Oil Flow Visualization", AIAA Paper 2016-1459, 2016.
[19] B. Vukasinovic, B., Glezer, A., Gordeyev, S., Jumper, E., Kibens, V., "Active Control and Optical Diagnostics of the Flow over a Hemispherical Turret", AIAA Paper 2008-0598, 2008.
[20] S.J. Beresh, J.F. Henfling, R.W. Spillers, B. O.M. Pruett, "Unsteady Shock Motion in a Transonic Flow over a Wall-Mounted Hemisphere", AIAA Paper 2013-3201, 2013.
[21] Liu T, Campbell BT, Burns SP, Sullivan JP, "Temperature- and pressure-sensitive luminescent paints in aerodynamics," Appl. Mech. Rev. 50(4), pp.227–246, 1997.
[22] Gregory JW, Asai K, Kameda M, Liu T, Sullivan JP, "A review of pressure-sensitive paint for high-speed and unsteady aerodynamics, " Proc Inst Mech Eng G J Aerosp 222(2), pp. 249–290, 2008.
[23] S. Fang, S,R. Long, K,J. Disotell, J,W. Gregory,F,C. Semmelmayer, and R.W. Guyton, "Comparison of Unsteady Pressure-Sensitive Paint Measurement Techniques," AIAA Journal, 50(1), pp. 109-122, 2012.
[24] S. Fang, K. J. Disotell, S.R. Long, J.W. Gregory, F.C. Semmelmayer, and R.W. Guyton, "Application of fast-responding pressure-sensitive paint to a hemispherical dome in unsteady transonic flow," Experiments in Fluids 50, pp. 1495–1505, 2011.
[25] N. De Lucca, S. Gordeyev, E. Jumper, K. Hird, T.J. Juliano, J.W. Gregory, J. Thordahl and D.J. Wittich, " The Estimation of the Unsteady Aerodynamic Force Applied to a Turret in Flight ", AIAA Paper 2013-3136, 2013.
[26] N. De Lucca, "Studies of The Pressure Field And Related Beam Jitter For Hemisphere-On-Cylinder Turrets", Ph.D. Thesis, University of Notre Dame, 2016.
[27] G. Berkooz, P. Holmes, and J.L. Lumley, "The proper orthogonal decomposition in the analysis of turbulent flows," Ann. Rev. Fluid Mech., 25, 539-575, 1993.
[28] P. Holmes, J.L. Lumley, and G. Berkooz, "Turbulence, Coherent Structures, Dynamical Systems and Symmetry", Cambridge University Press, 1996.
[29] J. Lumley, "Stochastic Tools in Turbulence", Academic, New York, 1970.
[30] N. De Lucca, S. Gordeyev, J. Morrida, E. Jumper, and D.J. Wittich, "Modal Analysis of the Surface Pressure Field Around a Hemispherical Turret using Pressure Sensitive Paint," AIAA Paper 2018-0932, 2018.
[31] Crafton, J., Forlines, A., Palluconi, S., Hsu, K-Y., Carter, C., and Gruber, M., "Investigation of transverse jet injections in a supersonic crossflow using fast-responding pressure-sensitive paint" Exp. Fluids 56: 27, 2015.
[32] K. Taira, S.L. Brunton, S.T.M. Dawson, C.W. Rowley, T. Colonius, B.J. McKeon, O.T. Schmidt, S. Gordeyev, V. Theofilis, and L.S. Ukeiley, "Modal Analysis of Fluid Flows: An Overview", AIAA Journal, 2017, https://doi.org/10.2514/1.J056060
[33] N. De Lucca, S. Gordeyev and E.J. Jumper, "Global Unsteady Pressure Fields Over Turrets In-Flight," AIAA Paper 2015-0677, 2015.
[34] E.R. Mathews, K.Wang, M.Wang, E.J. Jumper, "LES of an Aero-Optical Turret Flow at High Reynolds Number," AIAA paper 2016-1461, 2016,
[35] E.R. Mathews, "A Numerical and Theoretical Analysis of Aero-Optics With Application to an Optical Turret," Ph.D. thesis, University of Notre Dame, 2017.